



Andersson, S. M.L., Hou, L. , Marsh, J. H. and Farmer, C. D. (2020) Comparison of Cross-section Profile Designs for Integrated Polarization Mode Controllers. In: 5th International Conference on the UK-China Emerging Technologies (UCET 2020), Glasgow, UK, 20-21 Aug 2020, ISBN 9781728194882 (doi:[10.1109/UCET51115.2020.9205445](https://doi.org/10.1109/UCET51115.2020.9205445))

There may be differences between this version and the published version. You are advised to consult the publisher's version if you wish to cite from it.

<http://eprints.gla.ac.uk/221820/>

Deposited on 6 August 2020

Enlighten – Research publications by members of the University of Glasgow
<http://eprints.gla.ac.uk>

Comparison of Cross-section Profile Designs for Integrated Polarization Mode Controllers

Sia M. L. Andersson
James Watt School of Engineering
University of Glasgow
Glasgow, United Kingdom
s.andersson.1@research.gla.ac.uk

Dr. Lianping Hou
James Watt School of Engineering
University of Glasgow
Glasgow, United Kingdom
lianping.hou@glasgow.ac.uk

Prof. John H. Marsh
James Watt School of Engineering
University of Glasgow
Glasgow, United Kingdom
John.Marsh@glasgow.ac.uk

Dr. Corrie D. Farmer
Kelvin Nanotechnology Ltd
Glasgow, United Kingdom
corrie@kntnano.com

Abstract—Many laser applications in quantum technology require circularly polarized light at wavelengths accessible only through the GaAs-AlGaAs material system. Two proven designs of polarization mode convertor (PMC) were compared through simulation for a modified commercial 830 nm GaAs-AlGaAs structure. Structure type 1 used a deep-etched ridge waveguide, with a shallow-etched slot placed asymmetrically within the ridge. Structure type 2 also used a deep-etched ridge, but with sides of the ridge etched to different depths. Both structures support zero-order *TE* and *TM* modes, with the effective index difference between the modes determining the length of the PMC device. Although a range of dimensions and compositions was investigated, it was found the geometry of the waveguides did not significantly affect the effective index difference. The refractive index of the waveguide core was swept from 3.39 to 3.43, corresponding to Al contents from 0.45 to 0.3 respectively. In both structures, a higher index leads to the mode being concentrated in the core, which may lead to lower losses. As the structures give similar results, the main decider as to which one should be chosen should be the relative simplicity of fabrication.

Keywords—optical polarization; GaAs/AlGaAs; circular polarization, photonic integrated circuits, polarization mode control; PMC.

I. INTRODUCTION

Polarization is one of the key properties of electromagnetic radiation. Several designs of integrated polarization mode controller (PMC) have been reported over the past two decades. Asymmetric waveguides have been achieved through inclines, slots and periodically loaded waveguides, and applications have mostly focused on polarization multiplex in communications at the 1.55 μm wavelength [1-6]. New application areas for polarization control include the quantum technology field, where polarized light is used in precision measurement applications utilizing technologies such as atom cooling and coherent population trapping [7-8]. There is significant interest in scaling such systems from the size of an optical table down to integrated systems that are highly portable [9] for example an integrated polarization mode control component on a laser would negate the need for optical benches for one-beam atom cooling applications such as gMOT. [10]

For most quantum applications, the atom species typically used require wavelengths that are not accessible using InP material systems. These include 780 nm for the D2 hyperfine structure transition of R-87 and 894 nm for the D1 transition

of Cs-133. These wavelengths are accessible in the GaAs/AlGaAs material system.

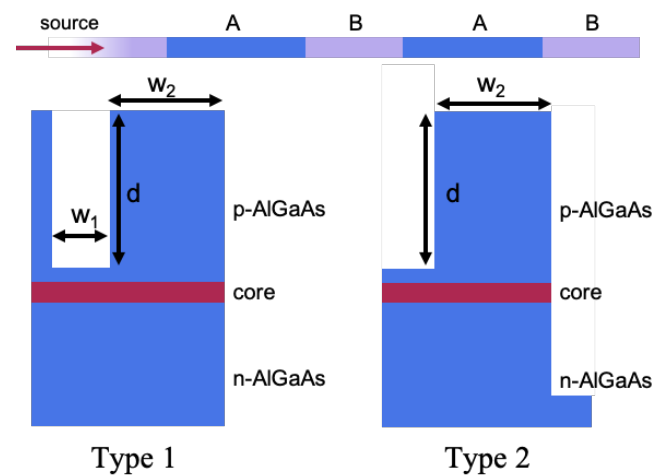


Fig. 1. Top: Overview of a typical PMC-DPS structure: PMC (device A) are placed alternating with DPS structures (B) to phase match and convert gradually for more control over the polarization. A typical PMC section would rotate optical axis orientation by an angle of 22.5° each. Bottom: Two PMC candidate structures.

	p-side material	Thickness	Doping
p-doped AlGaAs	GaAs cap	150 nm	Undoped
	$\text{Al}_{0.05}\text{Ga}_{0.95}\text{As} - \text{Al}_{0.45}\text{Ga}_{0.55}\text{As}$	120 nm	Zn
	$\text{Al}_{0.45}\text{Ga}_{0.55}\text{As}$	1900 nm	Zn
Core	$\text{Al}_{0.45}\text{Ga}_{0.55}\text{As} - \text{Al}_{0.3}\text{Ga}_{0.7}\text{As}$	135 nm	Undoped
	$\text{In}_{0.04}\text{Ga}_{0.96}\text{As}$	3.6 nm	Undoped
	$\text{Al}_{0.3}\text{Ga}_{0.7}\text{As} - \text{Al}_{0.45}\text{Ga}_{0.55}\text{As}$	135 nm	Undoped
n-side material	$\text{Al}_{0.45}\text{Ga}_{0.55}\text{As}$	2500 nm	Si
	GaAs	500 nm	Si
GaAs substrate			

Fig. 2. Key features of material simulated. GaAs/AlGaAs laser material at 830 nm modified from a commercially available structure. For simulating core refractive index effects, 120 nm of the layers on each side of the QW layer were altered in the range $n=3.39-3.43$.

As the precise dimensions and material properties of PMCs are critical, this article aims to present results on the effects of different material and design parameters on two different PMC structures, both based on mode-beating in asymmetric waveguide cross-sections. The first type is a reactive ion

etching (RIE) lag-based structure incorporating a slot into the waveguide. Due to RIE lag, the dry etch depth depends on the width of the feature such that a narrower feature etches to a shallower depth [1-2]. The second type is an asymmetrically deep-etched waveguide so that the etch depth is deeper on one side of the waveguide [11].

II. BACKGROUND AND METHOD

In order to generate new polarization states, PMCs are often paired with differential phase-matching sections (DPS), as illustrated in Fig. 1 where A represents a PMC and B represents a DPS. By including a series of these two sections in the linear waveguide, any point on the Poincaré sphere can be accessed, i.e. any polarization state can be achieved [12]. For many applications relevant to quantum technologies, the state of interest is circularly polarized light [7-8], which can be achieved by converting the linear polarization from the source (*TE* from a semiconductor laser) to 45° and then delaying the phase between the *TE* and *TM* components of the electrical field by π , giving circular polarization.

Waveguide asymmetry imposes birefringence on the light by offsetting the optical axis. This causes both of the fundamental polarization modes to be excited, leading to pronounced hybrid modes that display mode beating as they propagate along the waveguide.

The half-beat length $L_{1/2}$ in a passive PMC section is given by:

$$L_{1/2} = \frac{\pi}{\beta_1 - \beta_2} = \frac{\lambda}{2 \times \Delta n_{eff}} \quad (1)$$

where the half-beat length is the distance at which the beam has undergone a 90° rotation of polarization. Here, β_1 and β_2 are the propagation constants of the *TE* and *TM* modes respectively. To obtain the shortest PMC device, Δn_{eff} should be as large as possible. For circular polarization relevant to quantum applications, the quarter-beat length, $L_{1/4}$ which is half of the above, is the most interesting condition.

The simulations were done based on a separate confinement heterostructure (SCH) GaAs/AlGaAs laser with a single quantum well (QW) of InGaAs. The main features of the structure are illustrated in Fig. 2. The finite difference eigenmode (FDE) model implemented in Lumerical's MODE Solutions software was used to model the cross-section of the two types of structure.

Type 1 was a waveguide with a slot etched closer to one edge to introduce asymmetry. This type can be fabricated with the use of RIE lag in a single step as the etch depth depends on the width of the feature being etched. It is therefore possible to deep etch the waveguide and simultaneously produce a shallow-etched slot. For each slot width chosen, the depth of the slot is critical to the device performance, as even an over- or under-etch of 50 nm affects the conversion efficiency [1-2].

Type 2 was based on a recently reported PMC device in the InGaAsP/InP material system [11]. One side of the waveguide is more deeply etched than the other; one side is deep-etched and the etch depth on the shallower side is adjusted to give the conditions required for polarization mode control. The width of the waveguide w_2 was matched to the width of the remaining waveguide of type 1 for comparison purposes.

Effective index difference and resulting device length

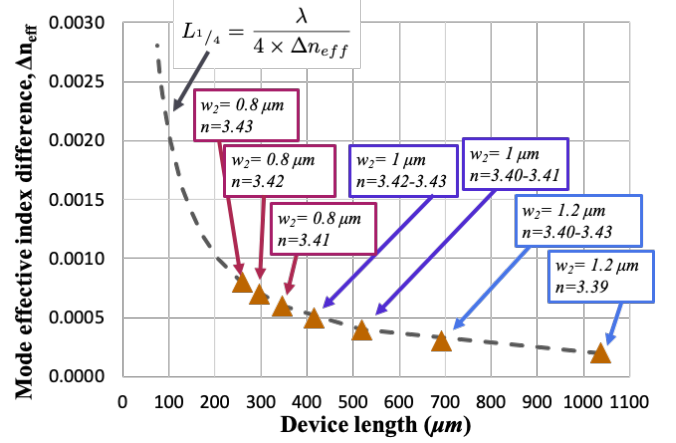


Fig. 3. Results of altering waveguide core refractive index for widths $w_2=0.8 \mu\text{m}$ (red), $1.0 \mu\text{m}$ (purple), $1.2 \mu\text{m}$ (blue) and $n=3.39-3.43$. The narrower devices required higher core n to achieve a conversion state. The shortest PMC device combines a narrow w_2 with high core n (see Fig. 2). Results for type 1 and 2 were the same in this respect.

It was investigated whether design choices in terms of parameters for geometry or material in the core affect Δn_{eff} . As the core (Fig. 2) consists of graded layers on each side of the QW, for the purposes of the simulation the layers were approximated as 15 nm of $\text{Al}_{0.3}\text{Ga}_{0.7}\text{As}$ on each side of the QW, and then 120 nm of $\text{Al}_{0.375}\text{Ga}_{0.625}\text{As}$ after each of those forming the waveguide core. These average layer compositions were used for modeling the refractive index effect, i.e. Al core content effect, on the PMC.

For parameters where the waveguide would support both modes equally, i.e. the polarization mode fraction between *TE* and *TM* is around 50/50, n_{eff} of each mode was recorded as well as the relevant geometric parameters. For type 1, a sweep was done with slot position and core refractive index. For type 2, a sweep was done of waveguide width and depth on the shallower side, as well as a core refractive.

III. RESULTS AND DISCUSSION

A. Slot structure (type 1)

For type 1, geometric variations of slot position and width (apart from design choices necessary to achieve the 50/50 mode support) have a negligible effect on Δn_{eff} .

The slot width was set to $w_1=420 \text{ nm}$ placed 180 nm from the waveguide edge. The depth of the slot was 2.05-2.26 μm . The width of the remaining waveguide was simulated for $w_2 = 1.2, 1.0$ and $0.8 \mu\text{m}$. It was found (Fig. 4) that smaller w_2 lead to higher Δn_{eff} . To achieve the conversion condition, a higher n_{core} was required for the narrower devices. The change in device length was dramatic, as $\Delta n_{eff} = 0.0002$ gives $L_{1/4}=1038 \mu\text{m}$ and $\Delta n_{eff} = 0.0008$ gives $L_{1/4}=257 \mu\text{m}$.

The refractive index n at the 830 nm wavelength was swept from 3.38 to 3.43 in the core as defined in Fig. 2. There was only negligible Δn_{eff} between the *TE* and *TM* mode, (Fig. 3). The dispersion of the mode was studied through the core confinement parameter.

As expected, the modal effective area shrunk with higher core refractive index. However, too strong a confinement would inhibit coupling between the *TE* and *TM* modes. In the lower refractive index region, the slot depth parameter d has

slightly more tolerance, but it may introduce more losses given that less of the mode is in the strongly guiding core.

B. Asymmetric waveguide structure (type 2)

For type 2, the waveguide width w_2 was set equivalent to w_2 for the type 1 waveguide. One side was deep-etched, and the other side had depths $d=2.05\text{-}2.26\ \mu\text{m}$, comparable to the slot depth d of type 1.

For $w_2=0.8, 1.0$ and 1.2 , Δn_{eff} and the mode effective area were found to be the same as for type 1, with a short device possible for $w_2=0.8$ and $n_{\text{core}} \sim 3.42$ (Fig. 3). Although the modal areas were similar for both structures, the fraction of the mode confined to the core was lower for type 2.

C. Fabrication considerations

As the two structures are fairly equivalent in terms of the parameters modelled for this project, the main decider as to which type and what parameters to choose would depend on the application intended for the device, as well as the fabrication techniques available.

Whilst the main attraction of the RIE lag type 1 structure is that it can be achieved through one deep dry etch process, the slot depth is a critical parameter with low tolerance: 20 nm discrepancy significantly reduces the conversion. However, if there is an established consistent process for deep etching and the RIE lag for the process is characterized type 1 is a viable option, especially if single step of etching for the PMC sections is desired. An example of such a structure and etch given in Fig.4.

Type 2 has the advantage that one side could be shallow-etched to the same depth as the DPS and other shallow-etched features the device may have, such as a laser. As this is a large area etch, its progress could be tracked with interferometry to gain the precise depth required. The other side of the waveguide could then be etched deep in a separate step. This would make the process more controllable, as a main disadvantage of the RIE lag approach is the requirement of a precise etch depth in the slot, where the depth cannot be tracked.

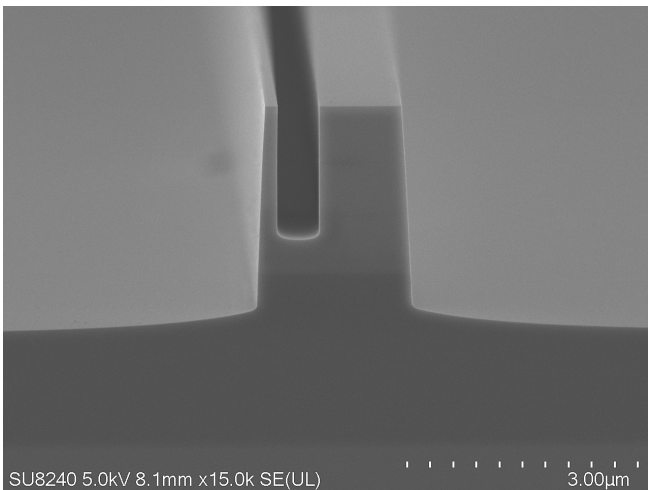


Fig. 4. Scanning electron microscope (SEM) image of a type 1 structure waveguide cross-section. Note the depth difference between the slot and surrounding waveguide, giving an RIE lag of around 900 nm.

IV. CONCLUSION

Two designs of the asymmetric waveguide cross-section of a PMC were simulated for integrating with an 830 nm GaAs/AlGaAs laser. Asymmetry was introduced in structure type 1 by etching a slot into the ridge waveguide that was placed to one side of the centerline of the ridge. In structure type 2, asymmetry was introduced by deep etching one side of the ridge and shallow etching the other. The refractive index of the waveguide core (other than the QW), was swept from 3.39 to 3.43 corresponding to Al contents of 0.45 to 0.3 respectively. In both structures, a higher index leads to the mode being confined more strongly in the core region. Aside from etch depths of the slot and shallow side of waveguide respectively, the width of the waveguide was found to be critical, in the case of type 1 the width of the portion where the mode propagates. The highest polarization mode conversion efficiency can be achieved with either type of structure at $w_2=0.8\ \mu\text{m}$ and $n_{\text{core}}=3.43$ where $\Delta n_{\text{eff}}=0.0008$, giving a PMC device length of 257 μm . In terms of the parameters studied here, both types cause the same mode behavior and convert with equal efficiency. Considering fabrication, type 2 has a significant advantage as the critical depth d is one side of the waveguide etch and a large feature which can be tracked to high accuracy through interferometry, whereas RIE lag is difficult to control. Further simulation is required to study other implications of the geometries of the two types.

ACKNOWLEDGEMENT

This work was supported by the Engineering and Physical Sciences Research Council (Grant number EP/L015323/1). The authors thank Prof David Hutchings and Dr. Kirsty Annand for valuable discussions. We also thank the staff and colleagues at the James Watt Nanofabrication Centre at the University of Glasgow for their help and hard work, and the staff of Kelvin Nanotechnology for fabrication discussions and support of Ms. Andersson.

REFERENCES

- [1] B. M. Holmes and D. C. Hutchings, "Realization of novel low-loss monolithically integrated passive waveguide mode converters," *IEEE Photonics Technol. Lett.*, vol. 18, no. 1, pp. 43–45, Jan. 2006.
- [2] M. A. Naeem, M. Haji, B. M. Holmes, D. C. Hutchings, J. H. Marsh, and A. E. Kelly, "Generation of High Speed Polarization Modulated Data Using a Monolithically Integrated Device," *IEEE J. Sel. Top. Quantum Electron.*, vol. 21, no. 4, pp. 207–211, Jul. 2015.
- [3] Z. Huan, R. Scarmozzino, G. Nagy, J. Steel, and R. M. Osgood, "Realization of a compact and single-mode optical passive polarization converter," *IEEE Photonics Technol. Lett.*, vol. 12, no. 3, pp. 317–319, Mar. 2000.
- [4] S. S. A. Obayya, B. M. A. Rahman, and H. A. El-Mikati, "Vector beam propagation analysis of polarization conversion in periodically loaded waveguides," *IEEE Photonics Technol. Lett.*, vol. 12, no. 10, pp. 1346–1348, Oct. 2000.
- [5] L. M. Augustin, J. J. G. M. van der Tol, E. J. Geluk, and M. K. Smit, "Short Polarization Converter Optimized for Active–Passive Integration in InGaAsP–InP," *IEEE Photonics Technol. Lett.*, vol. 19, no. 20, pp. 1673–1675, Oct. 2007.
- [6] J. J. Bregenzler, S. McMaster, M. Sorel, B. M. Holmes, and D. C. Hutchings, "Compact polarization mode converter monolithically integrated within a semiconductor Laser," *J. Light. Technol.*, vol. 27, no. 14, pp. 2732–2736, Jul. 2009.
- [7] P. Yun, S. Guérandel, and E. de Clercq, "Coherent population trapping with polarization modulation," *J. Appl. Phys.*, vol. 119, no. 24, p. 244502, Jun. 2016.
- [8] J. A. Rushton, M. Aldous, and M. D. Himsworth, "The feasibility of a fully miniaturized magneto-optical trap for portable ultracold quantum technology," *Rev. Sci. Instrum.*, vol. 85, no. 12, pp. 1–23, 2014.

- [9] M. Keil, O. Amit, S. Zhou, D. Groswasser, Y. Japha, and R. Folman, "Fifteen years of cold matter on the atom chip: promise, realizations, and prospects," *J. Mod. Opt.*, vol. 63, no. 18, 2016.
- [10] J. McGilligan, P. Griffin, R. Elvin, S. Ingleby, E. Riis and A. Arnold, "Grating chips for quantum technologies", *Scientific Reports*, vol. 7, no. 1, 2017.
- [11] M. Ito, K. Okawa, T. Suganuma, T. Tanemura, and Y. Nakano, "Monolithic Polarization Controller on Regrowth-Free InGaAsP/InP Platform with Strained MQW Layer," in *Optical Fiber Communication Conference (OFC) 2020*, 2020, p. T4H.4.
- [12] D. C. Hutchings and B. M. Holmes, "A waveguide polarization toolset design based on mode beating," *IEEE Photonics J.*, vol. 3, no. 3, pp. 450–461, 2011.